6-14-91 JS (2)

PREPARED FOR THE U.S. DEPARTMENT OF ENERGY,
UNDER CONTRACT DE-AC02-76-CHO-3073

PPPL-2757
UC-420,421,423,426

PPPL-2757

POWER AND PARTICLE BALANCE DURING NEUTRAL BEAM INJECTION IN TFTR

BY

C.S. PITCHER, R.V. BUDNY, K.W. HILL, S.J. KILPATRICK, D.M. MANOS, S.S. MEDLEY, AND A.T. RAMSEY

May 1991

PRINCETON
PLASMA PHYSICS
LABORATORY

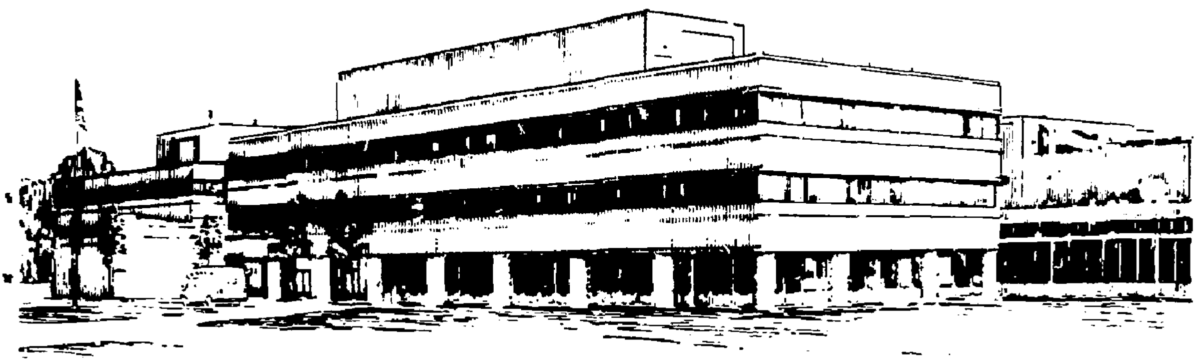

PRINCETON UNIVERSITY, PRINCETON, NEW JERSEY

Available to DOE and DOE contractors from the:

Office of Scientific and Technical Information
P.O. Box 62
Oak Ridge, TN 37831;
Prices available from (615) 576-8401.

Available to the public from the:

National Technical Information Service
U.S. Department of Commerce
5285 Port Royal Road
Springfield, Virginia 22161
703-487-4650

PPPL--2757

DE91 013459

Paper Submitted to the 9th International Conference on Plasma-Surface Interactions in Controlled Fusion Devices, 21-25 Bournemouth International Centre, U.K.

(last amended July 18, 1990)

Power and Particle Balance During Neutral Beam Injection in TFTR

C S Pitcher*, R V Budny, K W Hill, S J Kilpatrick, D M Manos, S S Medley and A T Ramsey

Princeton Plasma Physics Laboratory, Princeton University, Princeton, P.O. Box 451, NJ 08543, USA

* Canadian Fusion Fuels Technology Project, Toronto, Canada

Abstract

Detailed boundary plasma measurements on TFTR have been made during a NBI power scan in the range $P_{tot} = 1MW - 20MW$ in the L-mode regime. The behaviour of the plasma density $<n_e>$, radiated power P_{rad}, carbon and deuterium fluxes Γ_C, Γ_D, and Z_{eff} can be summarized as,

(1) $<n_e> \propto P_{tot}^{1/2}$

(2) $P_{rad}, \Gamma_C, \Gamma_D \propto P_{tot}$

(3) $Z_{eff} \sim constant$

It is shown that central fuelling by the neutral beams plays a minor role in the particle balance of the discharge. More important is the NBI role in the power balance. The TFTR data during NBI is consistent with a simple model of particle and power balance in which the particle sources originate primarily at the graphite limiter.

1 Introduction

It is nearly a universal observation on tokamaks with carbon limiters that the application of power, whether in the form of Ohmic, ICRF or neutral beam heating, results in increased influxes of deuterium and carbon from the limiter and a subsequent increase in the plasma density [1-4]. These effects are undesirable in that they make density and impurity control difficult, often resulting in a reduction of the potential thermonuclear yield of the discharge. These observations were shown to be consistent [4] with a simple model of power and particle balance put forward by McCracken [5] and based on,

(1) the balance of input power (P_{tot}) with radiated power (P_{rad}) and power conducted/convected to the limiter (P_{con})

(2) the balance of carbon sputtered from the limiter with that residing in the plasma and that redeposited on the limiter

What was not addressed in the McCracken model was the deuterium balance of the discharge, ie the balance between the deuterium held within the carbon limiter and that residing in the plasma. When this balance is also taken into account, as in [6], the three balance equations, ie for power, carbon and deuterium, predict the following behaviour for tokamak discharges in contact with a large-area carbon limiter:

(1) the influxes of deuterium Γ_D and carbon Γ_C, the radiated power and the edge electron density $n_e(a)$ all scale approximately linearly with the input power.

(2) the edge electron temperature $T_e(a)$ and Z_{eff} are approximately constant with input power.

(3) the average electron density of the discharge $< n_e >$ scales approximately as $P_{tot}^{1/2}$.

These scalings apply only to the case where the tokamak is sufficiently conditioned that the dominant impurity is carbon originating from physical sputtering and the dominant source of deuterium in the plasma-limiter system is the deuterium held within the graphite near-surface region before the discharge. This situation is often the case in TFTR which utilizes extensive conditioning and puffs or injects typically little deuterium gas in comparison to the inventory in the graphite (see Section 6).

It is the purpose of the present work to show that such scaling is obtained in TFTR during neutral beam injection in the L-mode regime. These discharges are without strong pre-depletion of deuterium from the graphite limiter so that the dominant particle source is the limiter. Such discharges follow energy confinement scaling presented by Goldston et al [7] and are coined "L-mode" discharges, as opposed to "Supershots", which result after extensive conditioning of the limiter to deplete it of deuterium [8]. This paper does not consider Supershots.

2 Experiment

TFTR has a major radius that is varied typically in the range $R_0 = 2.40m$ to $R_0 = 2.60m$ with a plasma cross-section which is essentially circular with corresponding minor radii of a = 0.75 m to a = 0.95 m. The plasma is limited by a toroidally symmetric inner bumper limiter composed of discrete graphite tiles covering an area of $\sim 22m^2$, Fig. 1. Typically, the area of the limiter wetted by the plasma is $\sim 6m^2$. The four neutral beam injectors on TFTR are capable of applying an input power of ~ 35 MW, but presently operate at powers of < 25 MW. This limit is set to some extent by the appearance of "carbon blooms", although recently the occurrence of blooms has been reduced by optimizing the shape of the limiter [9]. In addition to the core profile diagnostics on the tokamak, TFTR has a number of edge-specific diagnostics, including, a reciprocating Langmuir probe located approximately 37 cm above the outside midplane, a poloidal array of interference filter/telescopes which measure the poloidal D_α and C II (657.8 nm) distributions, an infra-red camera and a CCD camera plasma viewing system which obtains both the poloidal and toroidal distributions of emission from the low ionization states of deuterium and carbon. As is typical in most discharges in TFTR, the oxygen and metal levels are low and play little role in these discharges.

The spectral intensities of the low ionization states can be converted to particle influxes using theoretical photon efficiencies [10], if the local electron temperature is known. In general, because of surface heating limitations with the Langmuir probe at input powers > 5 MW, $T_e(a)$ is not routinely measured. For the analysis in this paper it is assumed that the edge temperature is independent of beam power, $T_e(a) \sim 50eV$. An approximately constant edge electron temperature with input power is predicted by the model [6] and is found on TFTR in the limited Langmuir probe data obtained at low power (see Section 5).

3 Time Evolution

Figure 2 shows the evolution of $P_{tot}, < n_e >, P_{rad}, Z_{eff}, \Gamma_C, \Gamma_D$ during a 1 s heating pulse at ~ 8 MW. Following the application of beam power, the discharge parameters rapidly evolve and reach, after typically ~ 0.3 s, a new equilibrium which is maintained for the duration of beam injection. The time to reach equilibrium τ_{eq} is set by the time for the injected energy to leave the plasma (the energy confinement time τ_E) and the time for deuterium and carbon released from the limiter to fill the plasma volume (the diffusion time τ_{DIFF}). The energy confinement time is generally short compared to 0.3 s, ie in the discharge shown in Fig. 2 $\tau_E \sim 0.12s$. The diffusion time can be estimated using the equation,

$$\tau_{DIFF} \sim \frac{a^2}{D} \qquad [1]$$

where D is the cross-field particle diffusion coefficient. From independent transport studies (see Section 7) D is found to be $\sim 2.3 m^2 s^{-1}$ and thus, with a minor radius of a = 0.95, we obtain $\tau_{DIFF} \sim 0.4s$ close to the experimentally observed τ_{eq}. Therefore, the time for the discharge to reach steady-state conditions appears to be determined by the plasma diffusion time.

As a result of the increased input power, the $< n_e >, P_{rad}, \Gamma_C$ and Γ_D reach new equilibrium values which are elevated above the Ohmic ones. The Z_{eff} of the discharge, however, is barely affected by the increase in power. The constant Z_{eff} is qualitatively consistent with the behaviour of the influxes at the limiter, ie, the carbon and deuterium influxes rise in proportion to each other, and thus it is reasonable to expect a constant Z_{eff}, given that carbon originating from the bumper limiter is the dominant impurity in the discharge. This argument assumes that the carbon ion transport does not change relative to the deuteron transport. It will be shown in Sections 6 and 7 that the beam fuelling of the discharge plays only a minor role in the particle balance and that the central densities of deuterium and carbon (and thus Z_{eff}) are determined to a large extent by the deuterium recycling influx Γ_D and carbon sputtering influx Γ_C, respectively.

For the data presented in this paper the average temperature rise of the limiter surface is below the threshold that can be detected by the infra-red camera (ie < 300 C). Such an upper limit for the surface temperature is consistent with simple one-dimensional thermal calculations based on the known thermal properties of the graphite, the input power to the plasma and the limiter wetted area. The low average temperature of the limiter, the absence of oxygen or significant hot spots (which at higher powers give rise to carbon blooms [9]) means that impurity production is dominated by physical sputtering at the graphite limiter. The fact that the carbon influx comes to a steady state value despite the continued application of power, Fig. 2, supports the conclusion that impurity production is not affected by surface temperature below this temperature threshold.

4 Scaling

The scaling of the steady-state values of $<n_e>, P_{rad}, \Gamma_C, \Gamma_D$ and Z_{eff} with input power appears in Fig. 3. Each data point represents conditions during the steady-state portion of a single discharge. As with the predictions from [6], the following approximate scalings are obtained,

$$<n_e> \propto P_{tot}^{1/2} \quad [2]$$

$$P_{rad}, \Gamma_C, \Gamma_D \propto P_{tot} \quad [3]$$

$$Z_{eff} \sim constant \sim 3.5 \quad [4]$$

The constant Z_{eff} was found in an earlier study on TFTR with the bumper limiter [11].

The carbon to deuterium flux ratio at the limiter is approximately constant, $\Gamma_C/\Gamma_D \sim 0.25$, consistent with the sputtering yields by deuterons and carbon ions being constant, as would be expected if $T_e(a) \sim constant$. However, the flux ratio value of 0.25 is significantly higher than can be explained by physical sputtering yields at normal incidence available in the literature. In a closed system, where all the carbon sputtered from the limiter returns to the limiter to self-sputter, the effective yield Y is [12]

$$Y \equiv \frac{\Gamma_C}{\Gamma_D} = \frac{Y_D}{1 - Y_C} = f[T_e(a)] \quad [5]$$

where Y_D, Y_C are the sputtering yields of deuterons and carbon ions on graphite [13]. If $T_e(a)$ is assumed to be ~ 50 eV and the carbon ion charge $Z_B = 3$, the appropriate incident deuteron and carbon energies are $5T_e(a) \sim 250eV$ and $11T_e(a) \sim 550eV$ [12], respectively. The expected effective yield is $Y \sim 0.05$, significantly less than found experimentally. Agreement can be obtained if the normal incidence sputtering yields Y_D, Y_C are enhanced by a number $\eta \sim 2$. The enhancement primarily affects the numerator in Eq. 5, as the carbon self-sputtering yield $Y_C \sim 0.8$ approaches unity.

It was argued theoretically and experimentally shown in [4] that the radiated power is directly proportional to the carbon influx,

$$P_{rad} = R_C \Gamma_C \quad [6]$$

where R_C is, effectively, the energy radiated per carbon atom entering the plasma. This number is expected to be a constant if the electron temperature and the product $<n_e> \tau_C$ (where τ_C is the carbon ion confinement time) are constant. It was shown in [4] that,

$$< n_e > \tau_C \propto \frac{(Z_{eff} - 1) < n_e >^2}{\Gamma_C}$$

From the results given in Fig. 3, this product is indeed approximately constant and a value of $R_C \sim 5keV/atom$ is obtained, which is in reasonable agreement with theory [14].

5 Langmuir Probe Data

Only a limited set of Langmuir probe data has been obtained during NBI due to over-heating of the probe elements when deeply immersed into the boundary plasma. Some results at low power neutral beam injection appear in Fig. 4. In this figure, the electron density n_e and temperature T_e profiles in the scrape-off layer (SOL) have been plotted for an Ohmic case with $P_{tot} = 1.1MW$ and with neutral beam heating with $P_{tot} = 3.0MW$. Within experimental uncertainty, no change in the edge electron temperature is observed during NBI with the value at the last closed flux surface (LCFS) being ~ 50 eV and the e-folding distance $\lambda_T \sim 6.5cm$. The Ohmic density e-folding distance of $\lambda_n \sim 5.9cm$ appears to reduce slightly with the application of power. The predominant change in the scrape-off layer as a result of increased power is an increase in the electron density by a factor of ~ 2.5. These measurements were obtained in different conditions than those of Fig. 3 but are qualitatively valid for most conditions in TFTR in that the main change is the edge density with little change in the edge electron temperature. Unfortunately, probe measurements into the LCFS at higher power input were not possible. It should be noted that Langmuir probe measurements of density are useful to obtain relative changes but give an absolute error of order ~ 2. These measurements are qualitatively similar to earlier observations in TFTR [15] although the absolute values of density and temperature are somewhat different, probably due to different machine conditions and different probe locations.

6 Graphite Deuterium Reservoir

The main point of this paper is to show that the predicted scaling [6] is obtained in TFTR during NBI in the L-mode regime. A crucial assumption in this model is that the main source of deuterium is that released from the graphite limiter. While this is obviously satisfied in the case of Ohmic and wave heating, for NBI heating, energetic deuterium atoms are purposely added to the discharge. Despite this, however, the dominant source of fuel for TFTR L-mode discharges is the recycling of deuterium from the graphite limiter. This fact is illustrated in Fig. 5, where the ratio of the sources of deuterium from the beams S_{NB} to that from recycling S_R (based on the spatially integrated D_α signal) is plotted as a function of beam power. This ratio is typically of order ~ 0.1 and weakly dependent on power. Similar results were obtained for NBI on JET [2,3]. In Supershot plasmas, where the limiter has been significantly depleted of deuterium, S_{NB}/S_R is larger, for example, ~ 0.3.

It is also clear that the amount of deuterium added to the system in the form of beam particles is negligible in comparison to the hydrogenic content of the combined plasma-limiter "reservoir". In fact, the plasma content is small compared to the content of the limiter reservoir, ie that region of the carbon that is in intimate contact with the plasma within an implantation distance (~ 20 nm) of incident boundary plasma deuterons. For example, at the highest input power the plasma content of deuterons is ~$6x10^{20}$, compared to the saturated limiter capacity of ~$2x10^{22}$. The fact that the beam particles have a negligible effect on the limiter inventory is clearly demonstrated by observing the $H_\alpha - D_\alpha$ composition of the recycling fuel during the course of a discharge. In the case of a carbon surface, deuterons striking the limiter are predominantly implanted rather than reflected [16] and reside in the carbon for a short period of time before they recombine to form molecules and are released back to the plasma. The $H_\alpha - D_\alpha$ intensity ratio is thus a measure of the hydrogenic composition within the material. The hydrogen is inherently present in the materials within the tokamak and thus also in the plasma. Figure 6 overlays the normalized $H_\alpha - D_\alpha$ lines at t = 2.8 s and t = 3.8 s, corresponding to the Ohmic phase and the end of the heating phase of the discharge illustrated in Fig. 2. The absolute signal during the heating phase is a factor of ~ 10 greater than during the Ohmic phase. As expected, the D signal relative to the H shows no increase despite the addition of only deuterium from the beams, strongly supporting the view that the beam source is negligible compared to the over-all inventory of the plasma-limiter system.

7 Simple Plasma Transport Model

Although the overall re-fuelling rate of the discharge is dominated by recycling of deuterium which is already present in the graphite before the start of the discharge, it is the beam injection which dominates the neutral fuelling of the centre of the discharge. The beam particles, although being small in number, penetrate to the magnetic axis while the recycling particles are ionized primarily in the boundary regions. This effect is demonstrated in Fig. 7 where the calculated source functions for deuterium for beam particles and for recycling are compared for a discharge with ~ 7 MW of beam heating. The machine conditions for this discharge (45803) were different than those present for the discharges given in Fig. 3, ie the limiter in 45803 had a somewhat lower deuterium content due to helium conditioning. The beam source profile is derived from the experimental density profiles and Z_{eff} using the SNAP code [17], while the recycling source profile is calculated by the Monte Carlo neutral transport code DEGAS [18] and normalized using the experimental $\dot{D}_\alpha$ measurements. As expected, when spatially integrated, the total source due to the beams is small, $\sim 6x\,10^{20} D\,s^{-1}$, compared to $\sim 4x\,10^{21} D\,s^{-1}$ for recycling; however, the beam particle source on-axis is two orders of magnitude larger than that from recycling.

To determine the relative contributions that the recycling and beam sources make to the central deuteron density (and thus the applicability of the scalings in the simple model contained in [6]) some assumption must be made regarding the particle transport in the plasma phase. We shall use a common prescription for particle continuity [19,20],

$$\frac{1}{r}\frac{d}{dr}\left[r\left(-D\frac{dn_e}{dr}+n_e v\right)\right]=I_D(r) \qquad [7]$$

where I_D is the deuteron source function and v is the inward pinch velocity given by

$$v=-SDr/a^2 \qquad [8]$$

where S is the inward pinch parameter, a constant.

The boundary condition for Eq. 7 can be obtained by relating the particle fluxes at the limiter (from experiment $\Gamma_D \sim 4x\,10^{21} D\,s^{-1}$, $\Gamma_C \sim 3x\,10^{21} C\,s^{-1}$) with the edge density $n_e(a)$,

$$\Gamma_D + Z_B\Gamma_C = \frac{1}{2} n_e(a) c_S A \qquad [9]$$

where $Z_B \sim 3$ is the average carbon ion charge in the SOL [21], $c_S \sim 4x\,10^4 m s^{-1}$ is the effective ion acoustic speed of the deuterium/carbon SOL plasma and A is the effective area of the flux tubes in the SOL,

$$A \sim \frac{4\pi a}{q_\psi}\lambda_\Gamma \qquad [10]$$

where $q_\psi \sim 4.6$ is the safety factor and $\lambda_\Gamma \sim 5cm$ is the e-folding distance for particle fluxes in the SOL derived from the Langmuir probe profiles. Substituting these quantities into Eqns. 9 and 10 we arrive at the boundary condition, $n_e(a) \sim 7x\,10^{18} m^{-3}$. This value is in reasonable agreement with the experimental data in Fig. 7, although the error in the derivation is probably a factor of ~ 2; the good agreement is thus probably fortuitous.

Equation 7 has been solved numerically using this boundary condition, the source functions given in Fig. 7b and fitted to the experimental density profile in Fig. 7a and additionally constrained by the experimental Z_{eff}~3.4 by adjusting the cross-field diffusion coefficient $D = 2.3m^2s^{-1}$ and the pinch parameter $S = 3$. Four theoretical curves are shown in comparison to the experimental density profile, ie using separately the beam source, the hydrogenic recycling source, no volume source (in this case the electrons are supplied solely by carbon) and the sum of the three. From this analysis, the beams contribute 18% to the central electron density, the fuel recycling 31% and carbon 51%. In terms of volume-average density $< n_e >$, the contribution of the beams is reduced, ie beams 13%, recycling 33% and carbon 54%. Thus, the discharge is to a large degree dominated by edge effects, ie the recycling of fuel and the production of carbon impurities at the limiter surface. The condition required for the applicability of the model, that the limiter is the dominant source of particles, is met. Beam fuelling plays only a minor role in the overall particle balance of the discharge. Similar results were obtained for NBI on JET [2,3]. These conclusions, of course, do not address the issue of fusion yield which depends only on deuteron densities and energies. In this respect, the beam contribution will be significant due in part to its contribution to the central deuteron concentration and in part due to suprathermal components in the plasma.

The diffusion coefficient D and the pinch parameter S are typical of those previously derived from impurity transport studies in TFTR using the laser blow-off technique [19]. In addition, the D is similar to the value required to explain the particle flux e-folding distance λ_Γ in the SOL; ie, using the values quoted above [22],

$$D \sim \frac{c_s \lambda_\Gamma^2}{2 q_\psi \pi R_0} \sim 1.4 m^2 s^{-1} \qquad [11]$$

8 Conclusions

In TFTR L-mode discharges the addition of neutral beam heating results in increased influxes of deuterium and carbon from the graphite limiter and a subsequent increase in the plasma density. This behaviour is in general undesirable in that the potential fusion yield of the discharge is reduced. The behaviour can be summarized by,

(1) $< n_e > \propto P_{tot}^{1/2}$

(2) $P_{rad}, \Gamma_C, \Gamma_D \propto P_{tot}$

(3) $Z_{eff} \sim constant$

Although it was not possible to routinely measure the edge electron temperature $T_e(a)$ in these discharges, the few existing measurements suggest a constant temperature with input power, ie $T_e(a)$~$50eV$. This constancy of $T_e(a)$ is consistent with the constant effective sputtering yield $Y \equiv \Gamma_C/\Gamma_D$ and constant Z_{eff}.

The above scalings observed on TFTR in the L-mode regime are in agreement with a simple model of power and particle balance [6] based on the assumption that the dominant source of deuterium is the graphite limiter. This implies two things for NBI in the L-mode regime. First, that the total amount of deuterium added in the form of beam particles is small in comparison to the total inventory in the graphite limiter. Second, that the central fueling is dominated by edge effects, ie fuel recycling and impurity production at the graphite limiter. On the latter point, although the beam particles penetrate to the centre of the discharge, their small number compared to the sum of recycling fuel and impurity production means that their contribution to the central plasma density is small. Recycling and impurity production at the boundary dominate the discharge simply due to overwhelming numbers. In Supershot plasmas in TFTR, through extensive conditioning of the limiter, the edge recycling can be reduced by a factor of ~ 3 compared with these results and in this case, central beam fuelling becomes more important.

Acknowledgements

This work was supported by U.S. Department of Energy Contract No. DE-AC02-76-CHO-3073 and No. DE-AC04-76DP00789. C S Pitcher is grateful for personal support from the Canadian Fusion Fuels Technology Project.

References

(1) S A Cohen, J Ehrenberg, T T C Jones et al, Plas Phys Cont Fusion 29 (1987) 1205.

(2) J Ehrenberg, J Nucl Mat 162-164 (1989) 63.

(3) T T C Jones, J W Cuthbertson, J Ehrenberg, A Gondhalekar, P D Morgan and J A Tagle, J Nucl Mat 162-164 (1989) 503.

(4) C S Pitcher, L deKock, J Ehrenberg et al, J Vac Sci Techn A 8, May/June (1990) 1760.

(5) G M McCracken, Plas Phys Contr Fus 29 (1987) 1273.

(6) C S Pitcher, Fusion Engineering and Design 12 (1990) 63.

(7) R J Goldston, Plas Phys Contr Fus 26 (1984) 87.

(8) J D Strachan, M Bitter, A T Ramsey et al, Phys Rev Lett 58 (1987) 1004.

(9) M Ulrickson, J Nucl Mat, proc. of 9th PSI Conference, Bournemouth, UK, 1990.

(10) K Behringer, H P Summers, B Denne, M Forrest and M Stamp, Plas Phys Contr Fus 31 (1989) 2059.

(11) M G Bell, V Arunasalam, M Bitter et al, Plas Phys Contr Fus 28 (1986) 1329.

(12) G M McCracken and P C Stangeby, Plas Phys Contr Fus 27 (1985) 1411.

(13) J Roth, private communication.

(14) P G Carolan and V A Piotrowicz, Plas Phys 25 (1983) 1065.

(15) D M Manos, S J Kilpatrick, M G Bell, R V Budny and M Ulrickson, J Nucl Mat 162-164 (1989) 251.

(16) W Eckstein and H Verbeek, IPP-Report 9/32 (1979), Max-Planck Institut für Plasmaphysik, D-8046 Garching/München, FRG.

(17) H Towner and R J Goldston, Bull Am Phys Soc 29 (1984) 1305.

(18) D H Heifetz et al, J Comput Phys 49 (1982) 309.

(19) B C Stratton, S A Cohen, F P Boody et al, J Nucl Mat 145-147 (1987) 587.

(20) R Simonini, J Spence and P C Stangeby, Contri Plas Phys 28 (1988) 459.

(21) G F Matthews, J Nucl Mat 162-164 (1989) 38.

(22) P C Stangeby, J A Tagle, S K Erents and C Lowry, Plas Phys and Contr Fus 30 (1988) 1787.

Table and Figure Captions

(1) Schematic cross-section diagram of the TFTR vessel showing the arrangement of the toroidal graphite bumper limiter, the reciprocating Langmuir probe and the poloidal D_α, C II telescope array.

(2) The time evolution of discharge 40932 during ~ 8 MW of neutral beam injection: $R_0 = 2.60m, a = 0.95m$, plasma current $I_p = 1.4MA$, toroidal magnetic field $B_T = 4T$.

(3) The scaling of plasma density $< n_e >$, radiated power P_{rad}, Z_{eff}, carbon Γ_C and deuterium Γ_D influxes from the limiter with total input power P_{tot}: discharges 40927 - 40945,$R_0 = 2.60m, a = 0.95m$, plasma current $I_p = 1.4MA$, toroidal magnetic field $B_T = 4T$.

(4) Boundary plasma profiles of density n_e and electron temperature T_e obtained with the reciprocating Langmuir probe in an Ohmic discharge (Ω) and a discharge with 2 MW of NBI. The total input powers of the two discharges where 1.1 MW and 3.0 MW, respectively: $R_0 = 2.45m, a = 0.80m$, plasma current $I_p = 1.4MA$, toroidal magnetic field $B_T = 4T$, $\Delta r \equiv r - a$.

(5) The ratio of fuelling sources as a function of total input power P_{tot} in the power scan (discharges 40927-40945). S_{NB} and S_R are the total fuelling rates for neutral beams and edge recycling, respectively: $R_0 = 2.60m, a = 0.95m$, plasma current $I_p = 1.4MA$, toroidal magnetic field $B_T = 4T$.

(6) The $H_\alpha - D_\alpha$ line-shapes during the Ohmic Ω and NBI phases of discharge 40932 (see Fig. 2). The signals at the two times have been normalized. The absolute intensity is ~ 10 times larger during NBI compared to the Ohmic phase: $R_0 = 2.60m, a = 0.95m$, plasma current $I_p = 1.4MA$, toroidal magnetic field $B_T = 4T$.

(7) Particle source and transport analysis of discharge 45803: (A) contributions to the electron density profile from beam particles, recycling fuel and carbon impurities, comparison of the sum of the three contributions with the experimental density profile obtained from the far infrared interferometer (B) the deuterium source functions for beam particles (from the SNAP code [17]) and for recycling (from the DEGAS code [18]): $P_{NB} = 6.7MW$ co-injection, $R_0 = 2.45m, a = 0.80m$, plasma current $I_p = 1.4MA$, toroidal magnetic field $B_T = 4T$.

#90X0221

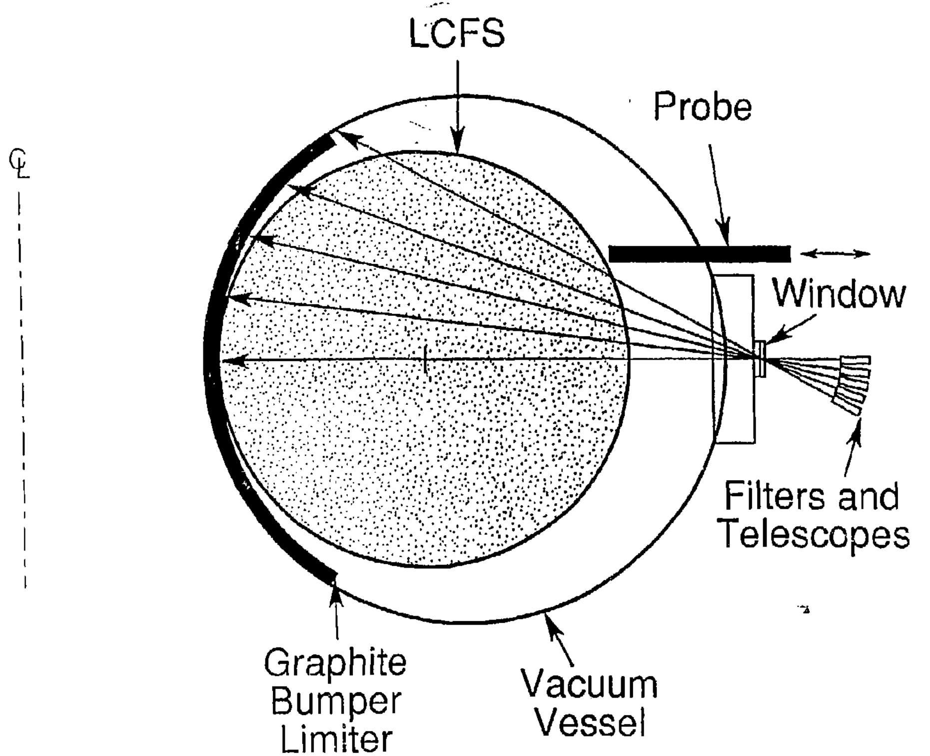

Fig. 1

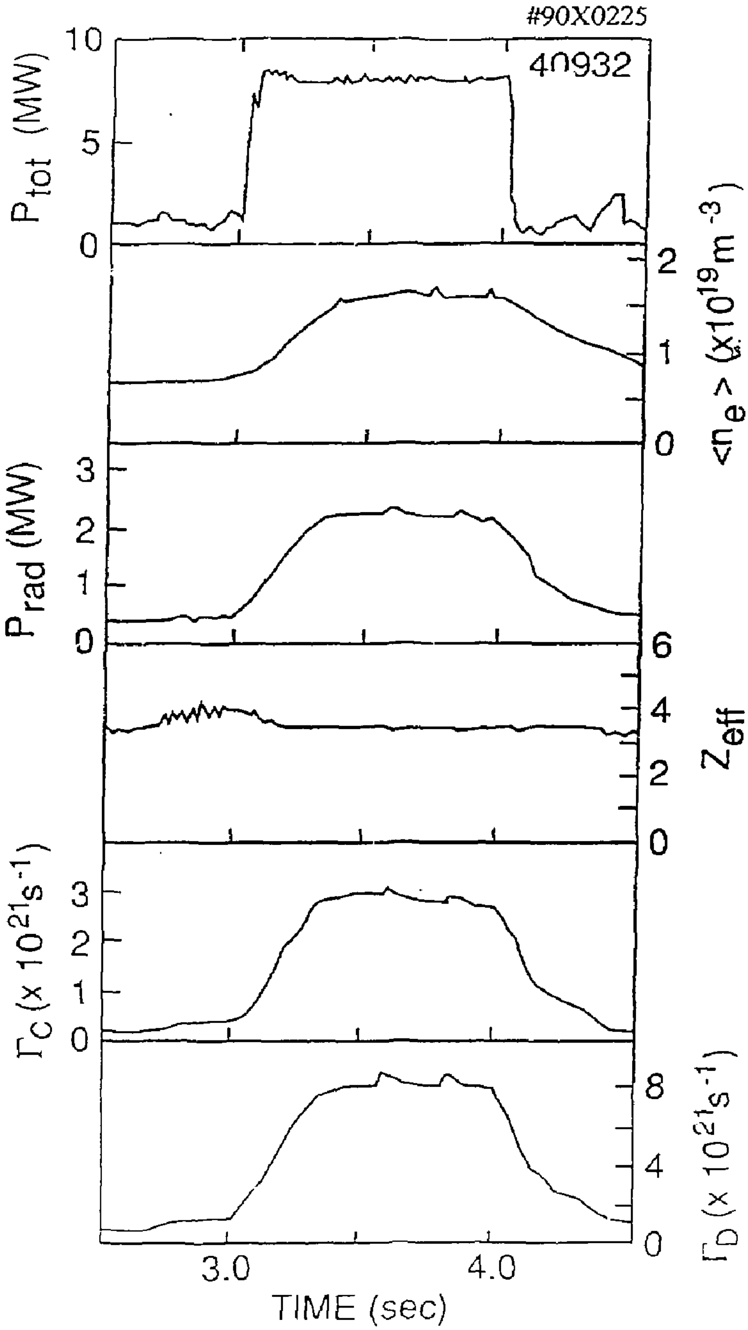
#90X0225
40932
P tot (MW)
10
5
0
<n e > (x10 19 m -3)
2
1
0
P rad (MW)
3
2
1
0
Z eff
6
4
2
0
Γ C (x 10 21 s -1)
3
2
1
0
Γ D (x 10 21 s -1)
8
4
0
3.0
4.0
TIME (sec)

Fig. 2

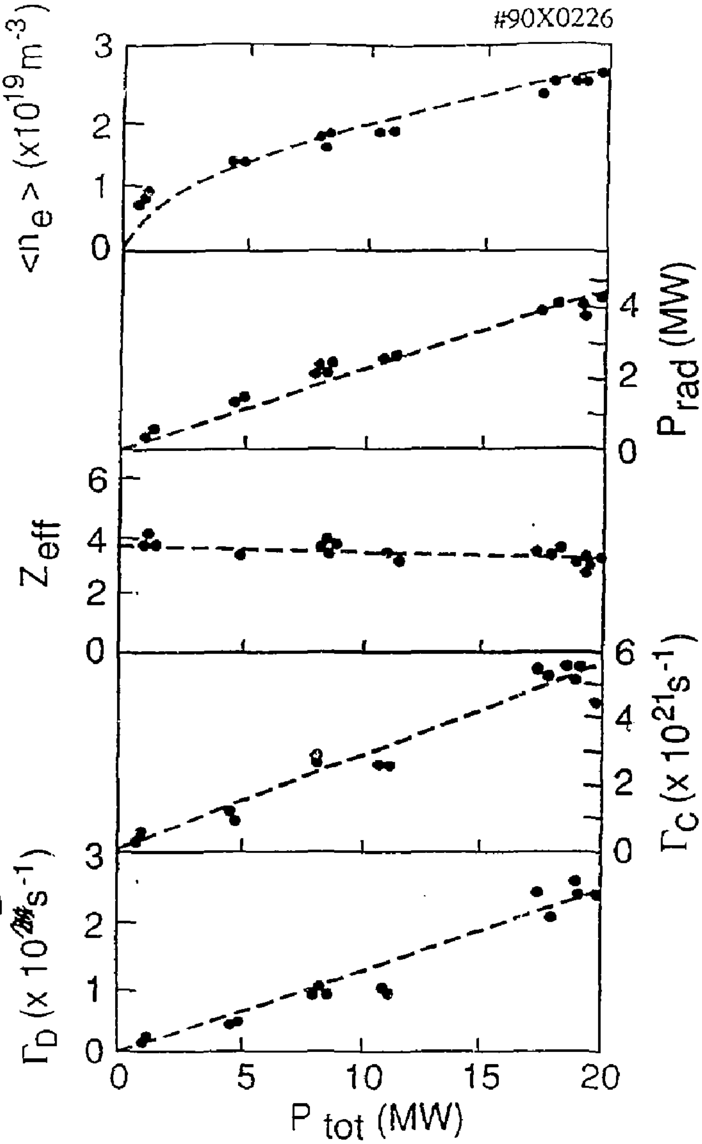
#90X0226
<n_e> (x10^19 m^-3)
P_rad (MW)
Z_eff
Γ_C (x 10^21 s^-1)
Γ_D (x 10^22 s^-1)
P tot (MW)
0
5
10
15
20

Fig. 3

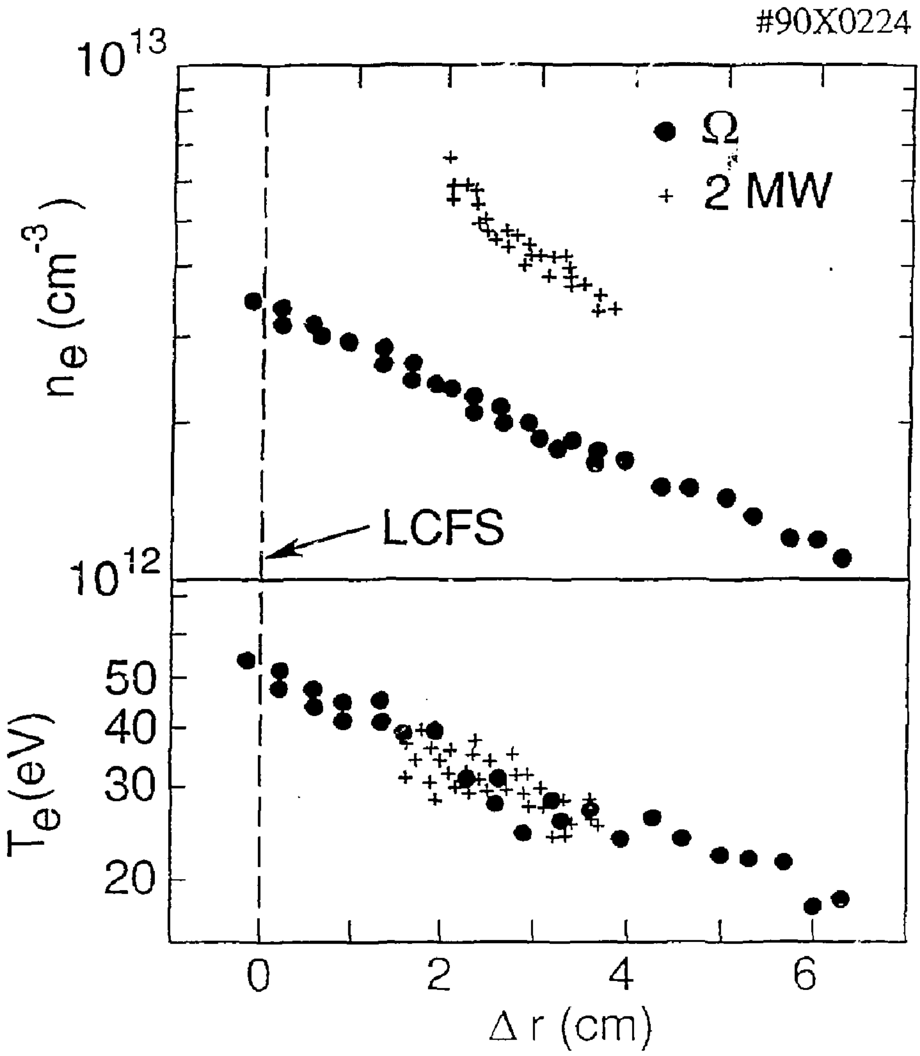

Fig. 4

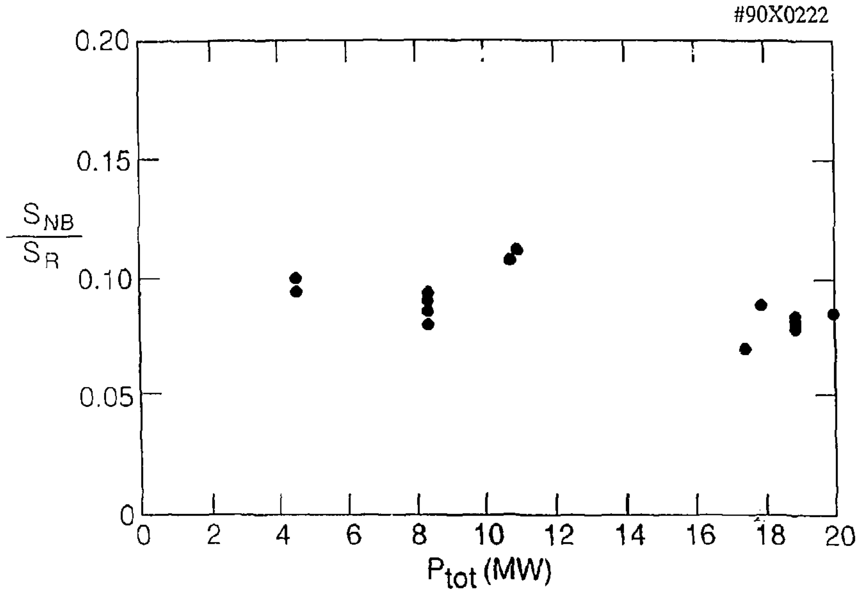
#90X0222
0.20
0.15
0.10
0.05
0
$\frac{S_{NB}}{S_R}$
0
2
4
6
8
10
12
14
16
18
20
P_{tot} (MW)

Fig. 5

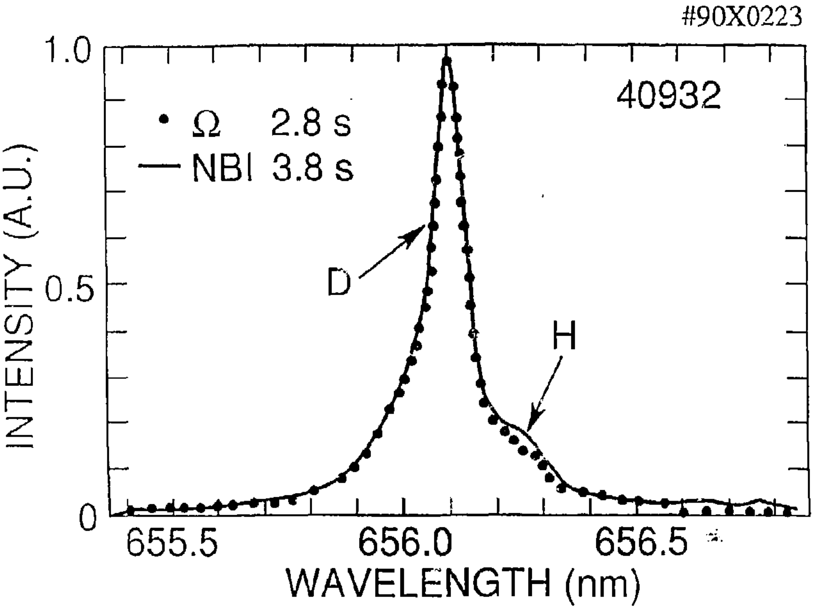
#90X0223
40932
• Ω 2.8 s
— NBI 3.8 s
D
H
1.0
0.5
0
655.5
656.0
656.5
INTENSITY (A.U.)
WAVELENGTH (nm)

Fig. 6

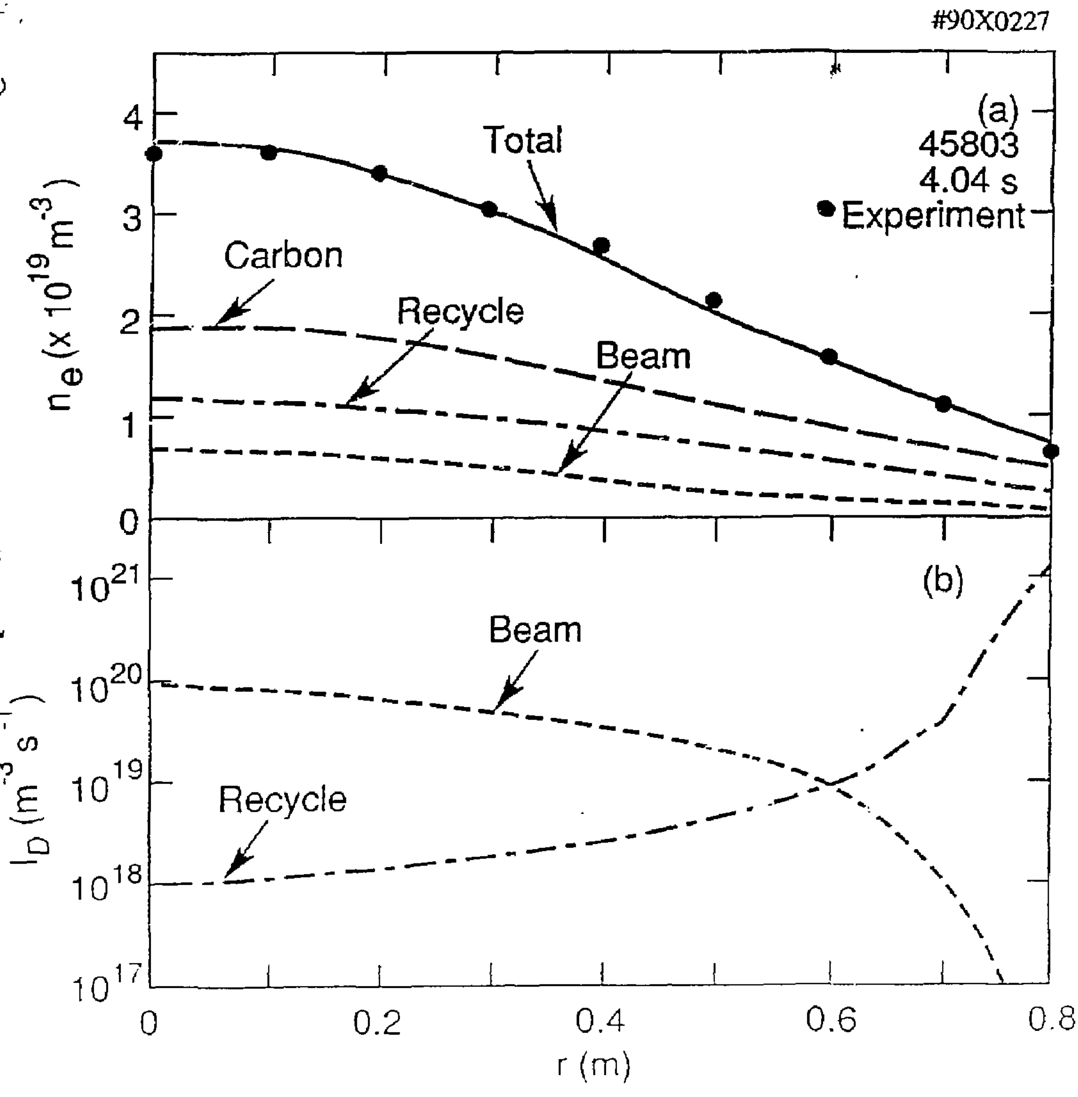
#90X0227
(a)
45803
4.04 s
Experiment
Total
Carbon
Recycle
Beam
$n_e (\times 10^{19} m^{-3})$
(b)
Beam
Recycle
$I_D (m^{-3} s^{-1})$
r (m)

Fig. 7